J. Mol. Biol. (1992) 228, 1193–1205

Nuclear Magnetic Resonance Solution Structure of Hirudin(1-51) and Comparison with Corresponding Three-dimensional Structures Determined Using the Complete 65-Residue Hirudin Polypeptide Chain

T. Szyperski[1], P. Güntert[1], S. R. Stone[2] and K. Wüthrich[1]

[1]*Institut für Molekularbiologie und Biophysik*
Eidgenössische Technische Hochschule-Hönggerberg
CH-8093 Zürich, Switzerland

[2]*University of Cambridge, Department of Haematology*
MRC Centre, Hills Road, Cambridge CB2 2QH, U.K.

(Received 26 May 1992; accepted 19 August 1992)

The three-dimensional structure of the N-terminal 51-residue domain of recombinant hirudin in aqueous solution was determined by ^{1}H nuclear magnetic resonance (NMR) spectroscopy, and the resulting high-quality solution structure was compared with corresponding structures obtained from studies with the intact, 65-residue polypeptide chain of hirudin. On the basis of 580 distance constraints derived from nuclear Overhauser effects and 109 dihedral angle constraints, a group of 20 conformers representing the solution structure of hirudin(1-51) was computed with the program DIANA and energy-minimized with a modified version of the program AMBER. Residues 3 to 30 and 37 to 48 form a well-defined molecular core with two antiparallel β-sheets composed of residues 14 to 16 and 20 to 22, and 27 to 31 and 36 to 40, and three reverse turns at residues 8 to 11 (type II), 17 to 20 (type II′) and 23 to 26 (type II). The average root-mean-square deviation of the individual NMR conformers relative to their mean co-ordinates is 0·38 Å for the backbone atoms and 0·77 Å for all heavy atoms of these residues. Increased structural disorder was found for the N-terminal dipeptide segment, the loop at residues 31 to 36, and the C-terminal tripeptide segment. The solution structure of hirudin(1-51) has the same molecular architecture as the corresponding polypeptide segment in natural hirudin and recombinant desulfatohirudin. It is also closely similar to the crystal structure of the N-terminal 51-residue segment of hirudin in a hirudin–thrombin complex, with root-mean-square deviations of the crystal structure relative to the mean solution structure of 0·61 Å for the backbone atoms and 0·91 Å for all heavy atoms of residues 3 to 30 and 37 to 48. Further coincidence is found for the loop formed by residues 31 to 36, which shows increased structural disorder in all available solution structures of hirudin, and of which residues 32 to 35 are not observable in the electron density map of the thrombin complex. Significant local structural differences between hirudin(1-51) in solution and hirudin in the crystalline thrombin complex were identified mainly for the N-terminal tripeptide segment and residues 17 to 21. These are further analyzed in an accompanying paper.

Keywords: hirudin; protein structure; nuclear magnetic resonance; hirudin–thrombin complex

1. Introduction

Hirudin variant HV1† occurs naturally in the salivary glands of the leech *Hirudo medicinalis* (Markwardt, 1970). It is a small protein of 65 amino

† Abbreviations used: HV1, hirudin variant 1; HV2-K47, hirudin variant 2 containing Lys in position 47; hirudin(1-51), the N-terminal 51-residue domain of hirudin variant HV1; NMR, nuclear magnetic resonance; 1D, 1-dimensional; 2D, 2-dimensional; NOE, nuclear Overhauser effect; NOESY, 2D nuclear Overhauser enhancement spectroscopy; COSY, 2D correlated spectroscopy; TOCSY, 2D total correlation spectroscopy; E.COSY, exclusive COSY; r.m.s.d., root-mean-square deviation; $^3J_{HN\alpha}$, vicinal spin-spin coupling constant between the amide proton and the α proton; $^3J_{\alpha\beta}$, vicinal spin-spin coupling constant between the α proton and one β proton; 2QF, 2-quantum filter; 3QF, 3-quantum filter; 2Q, 2-quantum; REDAC, use of redundant dihedral angle constraints; p.p.m., parts per million.

0022-2836/92/241193-13 $08.00/0

acid residues, and in the nuclear magnetic resonance (NMR) solution structure it is composed of a compact amino-terminal domain of residues 1 to 48 and a flexibly disordered carboxy-terminal tail of residues 49 to 65 (Folkers *et al.*, 1989; Haruyama & Wüthrich, 1989). Hirudin is most potent and most specific among the presently known inhibitors of the blood-clotting enzyme thrombin, a serine protease that plays a central role in the pathology of thrombotic diseases (Johnson *et al.*, 1989). Therefore, hirudin is well suited for therapeutic applications in cardiovascular medicine (Lent, 1986; Märki & Wallis, 1990).

Hirudin forms a stable 1 : 1 complex with thrombin, with a dissociation constant of 2×10^{-14} M (Stone & Hofsteenge, 1986). Recently, the X-ray crystal structures of thrombin (Bode *et al.*, 1989) and two hirudin–thrombin complexes (Grütter *et al.*, 1990; Rydel *et al.*, 1990, 1991) have been solved. The globular N-terminal domain of hirudin binds to the active-site cleft of thrombin, while the C-terminal tail, which is flexibly disordered in free hirudin in solution (Folkers *et al.*, 1989; Haruyama & Wüthrich, 1989), binds to the fibrinogen-binding exosite of thrombin and is well ordered in the complex (Grütter *et al.*, 1990; Rydel *et al.*, 1990, 1991). The novel inhibitor–protease interactions seen in the complex with thrombin suggest that hirudin represents a hitherto unknown family of serine protease inhibitors (Dodt *et al.*, 1985; Grütter *et al.*, 1990; Rydel *et al.*, 1990).

From comparison of the crystal structures of free and liganded thrombin it was possible to investigate structural changes of thrombin that occur due to the complex formation with hirudin (Rydel *et al.*, 1991). A corresponding investigation for hirudin has to rely on the NMR structure of free hirudin, since this protein has so far not been crystallized. NMR solution structures have been published for natural hirudin (Clore *et al.*, 1987), which contains a sulfated tyrosine residue in position 63, recombinant desulfatohirudin (Folkers *et al.*, 1989; Haruyama & Wüthrich, 1989) and the mutant Lys47 → Glu of recombinant desulfatohirudin (Folkers *et al.*, 1989). Obtaining a high-quality NMR structure of any of these intact hirudins turned out to be difficult because numerous intraresidual and sequential NOEs of the disordered carboxy-terminal tail are overlapped with NOEs of the amino-terminal core domain. We therefore studied a new protein corresponding to the N-terminal 51 residues of recombinant hirudin, hirudin(1-51) (Dennis *et al.*, 1990). In addition to enabling detailed comparisons with the corresponding domain of thrombin-bound hirudin in the previously reported 2·3 Å resolution (1 Å = 0·1 nm) X-ray crystal structure of a desulfatohirudin–thrombin complex (Rydel *et al.*, 1990, 1991), this new structure determination provided a basis for extensive physicochemical studies with hirudin (Szyperski, 1992). For example, it enabled assessment of the influence of the strongly acidic, flexible segment 52–65 on the static and dynamic properties of the hirudin core, and it was also the starting point for detailed studies of electrostatic interactions and surface hydrogen bonds in the globular domain.

2. Materials and Methods

(a) *NMR spectroscopy*

Hirudin(1-51) was produced by CNBr cleavage of the mutant Asn52 → Met of recombinant desulfatohirudin; it contains 52 residues, with position 52 occupied by homoserine (Dennis *et al.*, 1990). For the NMR experiments, 5 mM solutions were prepared in ^2H_2O, or in a mixed solvent of 90% water, 10% ^2H_2O. In the ^2H_2O solution, all labile protons were replaced with deuterium by keeping the sample at 40°C for 24 h and subsequent repeated lyophilization from ^2H_2O. All spectra were recorded at 22°C and pH 4·5, where the pH was adjusted by the addition of minute amounts of NaOH and HCl, or NaO^{2}H and ^{2}HCl, respectively. Two-dimensional ^{1}H NMR spectra were recorded on Bruker AM500 and Bruker AM600 spectrometers in the pure phase absorption mode with time-proportional phase incrementation (Marion & Wüthrich, 1983). Standard procedures were used to obtain complete ^{1}H resonance assignments: a 2QF-COSY spectrum (Rance *et al.*, 1983), a clean-TOCSY spectrum with a mixing time of 80 ms (Griesinger *et al.*, 1988), and a NOESY spectrum (Anil-Kumar *et al.*, 1980) with a mixing time of 100 ms were recorded in water. In addition, a 2Q-spectrum (Braunschweiler *et al.*, 1983) and a 3QF-COSY spectrum (Müller *et al.*, 1986) were recorded in ^2H_2O. The typical data size was 2048 points in t_2 and 512 points in t_1. The digital resolution after zero-filling was 3·0 Hz/point along ω_2 and 6·0 Hz/point along ω_1. For the collection of upper bound ^{1}H–^{1}H distances, 2 NOESY spectra with a mixing time $\tau_m = 50$ ms were recorded at 600 MHz with the following experimental conditions: (1) NOESY in water, recorded data size 960 points in t_1 and 4096 points in t_2, $t_{1max} = 65$ ms, $t_{2max} = 279$ ms, total measuring time about 50 h. (2) NOESY in ^2H_2O, recorded data size 786 points in t_1 and 4096 points in t_2, $t_{1max} = 60$ ms, $t_{2max} = 311$ ms, total measuring time about 50 h. The digital resolution after zero-filling was 1·8 Hz/point along ω_2 and 3·6 Hz/point along ω_1 for the NOESY spectrum recorded in water, and 1·6 Hz/point along ω_2 and 3·2 Hz/point along ω_1 in ^2H_2O. The residual water signal after preirradiation was further reduced using the convolution method of Marion *et al.* (1989*a*). Before Fourier transformation, the time domain data were multiplied with a sine-bell window function shifted by $\pi/2$ (DeMarco & Wüthrich, 1976). The 2 spectra were baseline-corrected in both dimensions using the program FLATT (Güntert & Wüthrich, 1992). Contributions arising from zero-quantum coherences were suppressed in the NOESY experiment recorded in ^2H_2O using the procedure described by Otting *et al.* (1990; see also Otting, 1990). The vicinal scalar coupling constants $^3J_{HN\alpha}$ were extracted from the aforementioned NOESY spectrum in water by inverse Fourier transformation of in-phase multiplets (Szyperski *et al.*, 1992*a*). In the same way, the scalar coupling constants $^3J_{\alpha\beta}$ for Thr, Ile and Val were obtained from the NOESY spectrum in ^2H_2O. The scalar coupling constants $^3J_{\alpha\beta}$ for the other residues were measured in an E.COSY spectrum (Griesinger *et al.*, 1985) recorded in ^2H_2O at 500 MHz.

For measurements of amide proton exchange rates, 450 µl of fully protonated 5 mM-protein solution at pH 4·5 was lyophilized. Subsequently, the protein was redissolved in the same amount of ^2H_2O. At 25 min after

preparation of the ^2H_2O solution, a series of 8 1D ^1H NMR spectra was recorded, and subsequently a series of 17 2D TOCSY spectra with a mixing time of 80 ms was accumulated starting, respectively 120, 205, 410, 498, 620, 790, 960, 1130, 4770, 5100, 5440, 12,240, 12,570, 14,940, 21,000, 23,360 and 31,280 min after preparation of the ^2H_2O solution. The first 4 2D spectra were recorded with 128 t_1 values and 2048 points in t_2, resulting in a measuring time of 85 min/spectrum. The remaining 2D spectra were recorded with 256 t_1 values and a measuring time of 170 min/spectrum. All spectra were recorded on a Bruker AMX 500 spectrometer using the method of Marion *et al.* (1989*b*) for quadrature detection in t_1. The time domain data matrix was expanded to 512 points in t_1 and 4096 points in t_2 by zero filling, and the final digital resolution along ω_2 was 3·0 Hz. Prior to Fourier transformation, the data were multiplied in both directions with a phase-shifted sine bell (De Marco & Wüthrich, 1976). The peak volumes in the 2D TOCSY spectra were integrated using the program EASY (Eccles *et al.*, 1991) and calibrated relative to well-separated cross-peaks of non-labile protons. Exchange rate constants were obtained from a least-squares fit of the experimental data to a single exponential function.

(b) *Structure determination and structure comparisons*

The strategy followed for the structure determination of hirudin(1-51) is closely similar to that for the structure determination of the *Antp*(C39 → S) homeodomain (Güntert *et al.*, 1991*b*). The program DIANA (Güntert *et al.*, 1991*a*) was used for the structure calculation from the NMR data, where the REDAC approach (Güntert & Wüthrich, 1991) was employed to improve convergence. The 20 DIANA conformers with the lowest final target function values were subjected to a restrained energy minimization using a modified version of the program AMBER (Singh *et al.*, 1986), which includes the same pseudoenergy terms for distance constraints and dihedral angle constraints as described by Billeter *et al.* (1990) and Widmer *et al.* (1989). Structure comparisons were performed as described by Billeter *et al.* (1989) and in the accompanying paper (Szyperski *et al.*, 1992*b*).

3. Results

(a) *Resonance assignments*

Sequence-specific ^1H NMR assignments for hirudin(1-51) were obtained with homonuclear 2D ^1H NMR experiments, following the standard strategy for small proteins (Billeter *et al.*, 1982; Wüthrich *et al.*, 1982; Wagner & Wüthrich, 1982; Wider *et al.*, 1982; Wüthrich, 1986) and using computer-support with the program EASY (Eccles *et al.*, 1991). A 3QF-COSY and a 2Q-spectrum recorded in ^2H_2O were used to complete the ^1H resonance assignments for the long side-chains. With few exceptions, the ^1H chemical shifts of hirudin(1-51) coincide with those of the corresponding hydrogen atoms in recombinant desulfatohirudin (Table 1). The analysis of the patterns of sequential and medium-range NOEs indicates that all regular secondary structure elements previously identified in recombinant desulfatohirudin (Folkers *et al.*, 1989; Haruyama & Wüthrich, 1989) are present also in hirudin(1-51).

(b) *Collection of conformational constraints*

NOE distance constraints were collected from two NOESY spectra recorded with a mixing time of 50 ms in a water or ^2H_2O solution of the protein. The NOE cross-peak volumes determined with the program EASY (Eccles *et al.*, 1991) were related to the corresponding proton–proton distances by the initial rate approximation (Gordon & Wüthrich, 1978; Wagner & Wüthrich, 1979; Anil-Kumar *et al.*, 1981). In total, 1070 NOEs were assigned in the two NOESY spectra, among which 580 NOEs represented effective conformational constraints, including 158 intraresidual, 159 sequential, 55 medium-range and 208 long-range distance constraints. No long-range or medium-range NOEs were observed for residues, 2, 33, 34, 36 or 49 to 51, indicating that the global positioning of the N-terminal dipeptide segment, the loop containing residues 33 to 36, and the C-terminal tripeptide segment is not well defined by the NMR data. The high number of sequential NOEs for residues 47 and 48 is in agreement with the formation of a polyproline helix II (Sasisekharan, 1959) by residues 46 to 48. For Leu13 and Leu30, where one β proton resonance was found to be degenerate with the γ proton resonance (Table 1), we referred the corresponding NOEs to the γ carbon atom and added a pseudoatom correction of 2·2 Å. Wherever the $^3J_{\alpha\beta}$ coupling constants indicated that multiple staggered rotamers are populated (Nagayama & Wüthrich, 1981), these $^3J_{\alpha\beta}$ values were not used to derive dihedral angle constraints, and distance constraints with the β protons were referred to the corresponding pseudoatom (Wüthrich *et al.*, 1983).

Overall, the input data set for the final structure calculation contained 109 dihedral angle constraints (39 to ϕ, 39 for ψ, and 31 for χ^1) in addition to the 580 NOE upper distance limits. Stereospecific assignments were obtained with the programs HABAS (Güntert *et al.*, 1989) and GLOMSA (Güntert *et al.*, 1991*a*,*b*) for 23 out of the 48 non-degenerate pairs of diastereotopic protons and for three pairs of isopropyl methyl groups (Table 1). In addition, the side-chain amide protons of three Asn and one Gln were individually assigned (Table 1). In the DIANA calculations, the three disulfide bonds 6–14, 16–28 and 22–39 were constrained by nine upper and nine lower distance limits (Williamson *et al.*, 1985). No hydrogen-bond constraints were used in the input for the present structure determination. A complete list of all conformational constraints has been submitted to the Brookhaven Data Bank, together with the atomic co-ordinates for hirudin(1-51), and the accession number is 1HIC.

(c) *Structure calculation*

For the final DIANA calculation using the REDAC strategy, the same parameters were used as in the structure calculation of the activation domain B described by Güntert & Wüthrich (1991), except that the maximal number of conjugate gradient

Table 1

Individual resonance assignments for pairs of diastereotopic substituents and side-chain amide protons in hirudin(1-51). Also listed are proton chemical shifts that differ by more than 0·05 p.p.m. from those previously reported for recombinant desulfatohirudin

	Chemical shift δ (p.p.m.)‡		
Residue†	αH	βH	Others
Val1		*1·90*	
Val2			γCH$_2$ 0·83, 0·88
Tyr3		2·65, 2·79	
Asp5		2·60, 2·75	
Cys6		2·67, 3·15§	
Ser9		3·96, 4·04	
Gly10	3·31, 4·60		
Gln11		2·29, 2·24	εNH$_2$ 7·82, 6·74
Asn12		2·89, 3·03	δNH$_2$ 7·48, 6·13
Leu13		*2·13, 1·61*	γCH *1·61*
Cys14		3·38, 3·12	
Leu15		2·02, 1·41	δCH$_3$ 0·83, 0·50
Cys16		2·84, 3·86	
Glu17			γCH$_2$ *2·05, 2·05*
Gly18	3·68, 3·92		
Ser19		4·01, 3·92	
Asn20		3·06, 2·57	δNH$_2$ 7·55, 7·07
Cys22		3·20, 2·91	
Gly25	3·62, 4·25		
Asn26		2·67, 2·74	
Cys28		2·86, 2·95	
Leu30		*1·57, 1·43*	*1·43*
Glu35		2·12, 2·19	
Lys36		1·77, 2·01	
Asn37			δNH$_2$ 7·91, 7·11
Gln38		1·96, 1·78	
Cys39		2·79, 3·15	
Val40			γCH$_3$ 0·91, 0·85
Pro46		1·90, 2·24	
Lys77			ζNH$_3^+$ *8·45*
Pro48		1·91, 2·35	
hSer52‖	*4·25*	*1·90, 2·12*	γCH$_2$ *3·68, 3·68, backbone NH, 8·42*

† Only those residues are listed for which individual assignments were obtained for at least 1 pair of diastereotopic substituents or side-chain amide protons, or for which at least 1 chemical shift value at 22 °C and pH 4·5 deviates by more than 0·05 p.p.m. from the corresponding value in desulfatohirudin (Haruyama & Wüthrich, 1989).

‡ For individually assigned (underlined) diastereotopic pairs of methylene protons or isopropyl methyl groups, the first value is the chemical shift of the proton or methyl group with the lower branch number, e.g. the β^2 hydrogen atom in β-methylene groups, or the γ^1 methyl group in Val. For the side-chain amide protons of Asn and Gln, the first value is the chemical shift of the proton that has a smaller distance from the nearest methylene carbon atom (C^β for Asn, C^γ for Gln). The chemical shifts that differ by more that 0·05 p.p.m. from those reported by Haruyama & Wüthrich (1989) for the corresponding hydrogen atoms in recombinant desulfatohirudin are printed in italics.

§ Due to a misprint, this chemical shift is erroneously reported as 2·77 p.p.m. in Table I of Haruyama & Wüthrich (1989), while in Table II of the same publication the correct value is given.

‖ The presence of homoserine 52 is due to CNBr-cleavage at position 52 (Dennis *et al.*, 1990). No stereospecific assignments were obtained for this residue.

iterations was slightly reduced, and that in the second REDAC step, $C^{(2)}$ (see Fig. 1 in Güntert & Wüthrich, 1991), the maximal target function value per residue for locally acceptable segments was 0·1 Å^2. Of the 50 calculations, 49 converged with a final target function value of less than 0·9 Å^2. The complete DIANA calculation for all 50 starting structures took 27·4 minutes of central processor unit time on a Cray Y-MP computer. The best 20 of the 50 DIANA conformers had very small residual distance constraint and dihedral angle constraint violations (Table 2). The relatively low AMBER

Table 2

Analysis of the 20 best DIANA conformers of hirudin(1-51) before and after restrained energy minimization with the program AMBER

Quantity	Average value ± standard deviation (range)†			
	Before energy minimization		After energy minimization	
DIANA target function (Å²)‡	0·12±0·03	(0·08 . . . 0·17)		
AMBER energy (kcal/mol)§	−197±45	(−280 . . . −84)	−654±40	(−750 . . . −592)
Residual NOE distance constraint violations:				
Number >0·2 Å	0		0	
Sum (Å)	1·0±0·2	(0·6 . . . 1·4)	2·7±0·2	(2·4 . . . 3·0)
Maximum (Å)	0·09±0·02	(0·06 . . . 0·16)	0·09±0·0	(0·08 . . . 0·10)
Residual dihedral angle constraint violations:				
Number >5°	0		0	
Sum (deg.)	3·2±0·7	(2·0 . . . 4·3)	17·5±3·4	(12·4 . . . 26·7)
Maximum (deg.)	0·9±0·1	(0·6 . . . 1·1)	2·5±0·4	(1·8 . . . 3·8)

A total of 50 structures were calculated with DIANA, but only the 20 structures with the smallest final target function values were subjected to energy minimization (see text).

† For the two groups of 20 conformers.

‡ The weighting factors for the NOE and hydrogen bond distance constraints were 1, for the van der Waals lower distance limits 2, and for dihedral angle constraints 5 Å². For the structures after energy minimization, the DIANA target function is not defined because these structures do not have the ECEPP standard geometry.

§ 1 cal = 4·184 J.

energies of these conformers before energy minimization indicated that most steric overlaps were successfully removed by DIANA. For each of these DIANA conformers, AMBER was able to find a low-energy conformation with nearly identical molecular geometry, with only a small increase of the sum of constraint violations (Table 2). The average of the 20 pairwise r.m.s.d. values between corresponding conformers before and after energy minimization is 0·21(±0·05) Å for the backbone atoms N, C^{α} and C′, and 0·29(±0·07) Å for all heavy atoms in the complete polypeptide chain 1–51.

(d) *The solution conformation of hirudin(1-51)*

A visual impression of the quality of the structure determination for hirudin(1-51) is afforded by Figure 1B, which shows the polypeptide backbone of the final group of 20 energy-refined DIANA conformers after superposition of the backbone

Table 3

Quantitative characterization of the structure determination of hirudin(1-51) by NMR in solution and comparison with the corresponding polypeptide segment in the X-ray crystal structure of a hirudin–thrombin complex

Atoms used for the comparison†	r.m.s.d. (Å)	
	⟨NMR⟩−NMR‡	⟨NMR⟩−X-ray‡
Backbone atoms N, C^{α}, C′ (1–51)	0·90±0·19	
All heavy atoms (1–51)	1·40±0·19	
Backbone atoms N, C^{α}, C′ (3–30; 37–48)	0·38±0·07	0·61
Same + best defined side-chains§	0·48±0·07	0·84
All heavy atoms (3–30; 37–48)	0·77±0·07	0·91‖

† The numbers in parentheses denote the protein segments considered in the comparison. For the superposition, the r.m.s.d. was calculated for the backbone atoms of this segment in all cases.

‡ ⟨NMR⟩ denotes the average co-ordinates of the 20 conformers that represent the solution structure of hirudin(1-51) (see Materials and Methods), NMR the individual 20 energy-refined DIANA conformers, and X-ray the conformation of the corresponding residues in the crystal structure of the HV2-K47-thrombin complex by Rydel *et al.* (1990, 1991). The locations of residues 32 to 36 of hirudin are not reported in the X-ray crystal structure.

§ Includes the backbone atoms N, C^{α} and C′ of residues 3 to 30 and 37 to 48 and the side-chain heavy atoms of the 19 best-defined ones among these residues, i.e. residues 4, 5, 6, 7, 9, 12, 14, 15, 16, 19, 20, 22, 26, 28, 29, 39, 40, 46 and 48.

‖ For residues 1 to 32 and 36 to 51 the amino acid sequence of hirudin(1-51) deduced from hirudin variant HV1 differs in 5 positions from that of recombinant hirudin variant HV2-K47 present in the X-ray crystal structure of the hirudin–thrombin complex reported by Rydel *et al.* (1990, 1991). For those 5 residues only the heavy atoms that are present in both hirudin variants were used for the calculation of the r.m.s.d. value. The co-ordinates of the γ and δ-carbon atoms of Glu43 were not reported for the X-ray crystal structure.

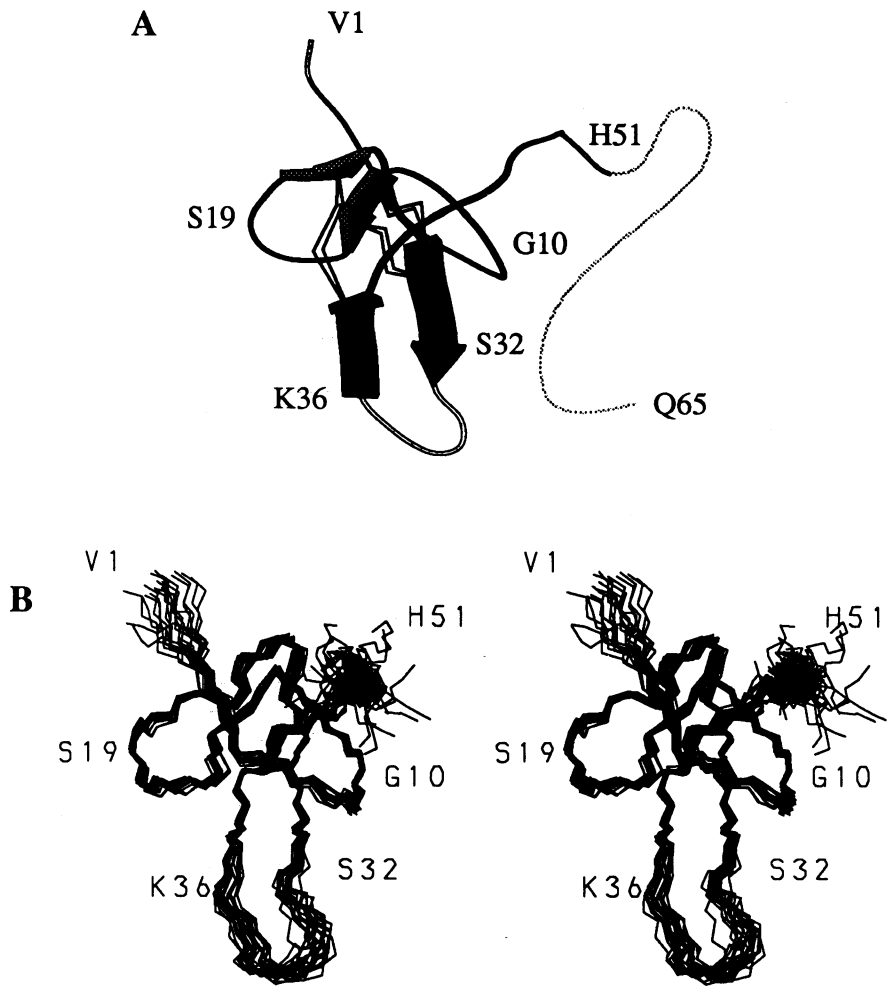

Figure 1. A, Reconstruction of the intact hirudin polypeptide chain using the atomic co-ordinates of the DIANA conformer of hirudin(1-51) with the lowest target function value for residues 1 to 48 and previous knowledge that segment 52–65 is flexibly disordered (Folkers *et al.*, 1989; Haruyama & Wüthrich, 1989). The Figure shows a schematic ribbon drawing of recombinant desulfatohirudin generated with the program MOLSCRIPT (Kraulis, 1991). The arrowed ribbons indicate position and direction of the β-sheet strands. A black rope represents the well-structured loop areas. Residues 1 to 2, 32 to 36 and 49 to 51, which are constrained only poorly, by the NMR data for hirudin(1-51), are indicated by a white rope, and residues 52 to 65 by a dotted line. B, Stereo view of the polypeptide backbone of the 20 energy-refined DIANA conformers of hirudin(1-51) used to represent the NMR structure in solution. Conformers 2 to 20 were superimposed for pairwise minimum r.m.s.d. of the backgone atoms N, C^{α} and C′ of residues 3 to 30 and 37 to 48 with conformer 1. In both drawings the protein core 1–48 is shown in the same orientation, and some positions have been identified with the 1-letter amino acid symbol and the sequence location.

atoms N, C^{α} and C′ of residues 3 to 30 and 37 to 48 for minimal r.m.s.d. The r.m.s.d. values calculated for different selections of atoms (Table 3) confirm that a high-quality structure of hirudin(1-51) was obtained, which includes, however, three disordered regions with residues 1 to 2, 31 to 36 and 49 to 51. Figure 1A presents a reconstruction of the intact, 65-residue hirudin molecule based on the NMR structure co-ordinates for hirudin(1-51) (see the legend to Fig. 1 for details). It identifies the location of the well-structured parts of hirudin(1-51) in intact hirudin, the spatial positions of the three disulfide bonds 6–14, 16–28 and 22–39, and the locations of the two antiparallel β-sheets with residues 14 to 16 and 20 to 22, and 27 to 31 and 36 to 40, respectively. The C-terminal segment 49–65 is in a flexibly disordered, predominantly extended form (Folkers *et al.*, 1989; Haruyama & Wüthrich, 1989). Background information for a more detailed characterization of the molecular structure is presented in Table 4, which lists the hydrogen bonds identified in the NMR solution structure of hirudin(1-51), and in three Figures. Figure 2 shows plots of atomic displacements for individual amino acid residues or short peptide segments *versus* the sequence. Figure 3 gives a survey of the precision with which the individual dihedral angles ϕ_i, ψ_i and χ_i^1 were determined. Finally, a visual display of the structural order and disorder in the individual amino acid side-chains is afforded by Figure 4.

Inspection of the hirudin(1-51) backbone structure starting from the N terminus shows that the somewhat disordered residues 1 and 2 are followed by a well-defined heptapeptide segment with irregu-

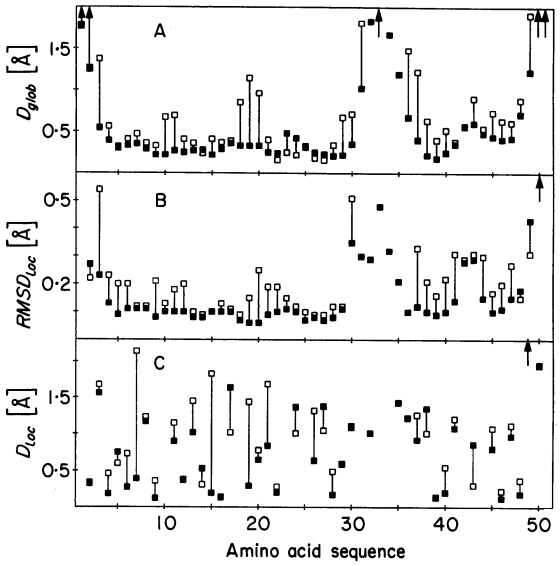

Figure 2. The following parameters are plotted *versus* the amino acid sequence of hirudin(1-51). A, The mean of the backbone displacements, D_{glob}, of the 20 energy-minimized DIANA conformers relative to the mean NMR structure (filled squares), and the backbone displacements, D_{glob}, of hirudin in the X-ray crystal structure of the thrombin complex relative to the mean NMR structure (open squares). B, The mean of the local r.m.s. deviations $RMSD_{loc}$, for the backbone superposition of all tripeptides along the sequence relative to the mean NMR structure (filled squares), and the corresponding local r.m.s.d. values of hirudin in the X-ray crystal structure of the thrombin complex relative to the mean NMR structure (open squares); the r.m.s.d. values for the tripeptides are plotted at the position of the central residue. C, The mean of the side-chain displacements, D_{loc}, of the 20 energy-minimized DIANA conformers relative to the mean NMR structure (filled squares), and the corresponding displacements for hirudin in the X-ray crystal structure of the thrombin complex relative to the mean NMR structure (open squares). The arrows indicate values that go off-scale.

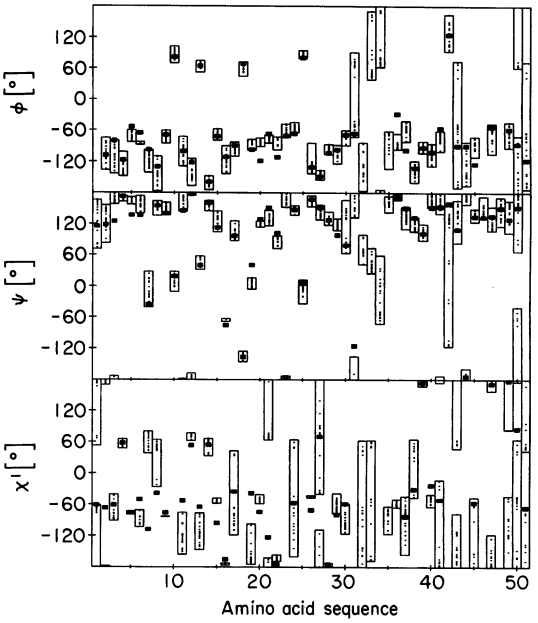

Figure 3. In plots *versus* the amino acid sequence the dihedral angles ϕ, ψ and χ^1 (from top to bottom) observed for hirudin in the crystal structure of the hirudin–thrombin complex (filled rectangles) are compared with the range of the dihedral angle values found in the 20 energy-refined DIANA conformers of hirudin(1-51) (open bars). Within the bars, the values for the dihedral angles in the 20 individual energy-refined DIANA conformers are indicated as dots. The dihedral angles of residues 32 to 35 of hirudin were not reported for the crystal structure (Rydel *et al.*, 1990, 1991).

lar secondary structure. A reverse turn at residues 8 to 11 is of type II (Chou & Fasman, 1977; Crawford *et al.*, 1973), and is connected *via* a kink at residues 12-13 with the first β-strand. The two strands of the first β-sheet are connected by a type II′ reverse turn consisting of residues 17 to 20, and the link between the two β-sheets forms a type II turn at residues 23 to 26. The three reverse turns 8–11, 17–20 and 23–26 are well determined by the NMR data, as evidenced by the small values of D_{glob} and $RMSD_{loc}$ in Figure 2. Furthermore, Table 1 shows that stereospecific assignments were obtained for the α protons of Gly10, Gly18 and Gly25, and the hydrogen bond between residues 17 and 20 in the type II′ turn is also well defined (Table 4). In contrast, significantly increased global and local r.m.s.d. values (Figs 1 and 2) were obtained for most residues in the loop 31–36, which connects the two strands of the second β-sheet. The definition of this chain reversal by the NMR data differs from that in the lower-quality structures described earlier for natural hirudin (Clore *et al.*, 1987) or desulfatohirudin (Folkers *et al.*, 1989; Haruyama & Wüthrich, 1989) in that one contiguous group of conformations was obtained. The large local r.m.s.d. values for the backbone atoms of residues 30 to 35 (Fig. 2B) and the large ranges of values for the backbone dihedral angles of residues 31 to 34 (Fig. 3) show that the increased disorder cannot simply be attributed to a hinge motion, for example, about an axis through residues 31 and 36. (Note, for comparison, that although increased conformational disorder is observed for the N-terminal tripeptide segment (Fig. 1B), the small local r.m.s.d. values for the backbone atoms of these residues (Fig. 2B) indicate that the *local* structure is nonetheless well defined, and for all 20 energy-refined DIANA conformers the ranges of the ϕ and ψ angles for these residues (Fig. 3) are close to the values typically observed in β-sheets.) The polypeptide segment 41–45 following the second β-sheet exhibits somewhat increased atomic displacement values (Fig. 2A), indicating local conformational disorder, but residues 46 to 48 form a short stretch of polyproline helix II (Sasisekharan, 1959; Yonath & Traub, 1969), which is again well characterized by the NMR data. The high atomic displacements and local r.m.s.d. values for the C-terminal tripeptide

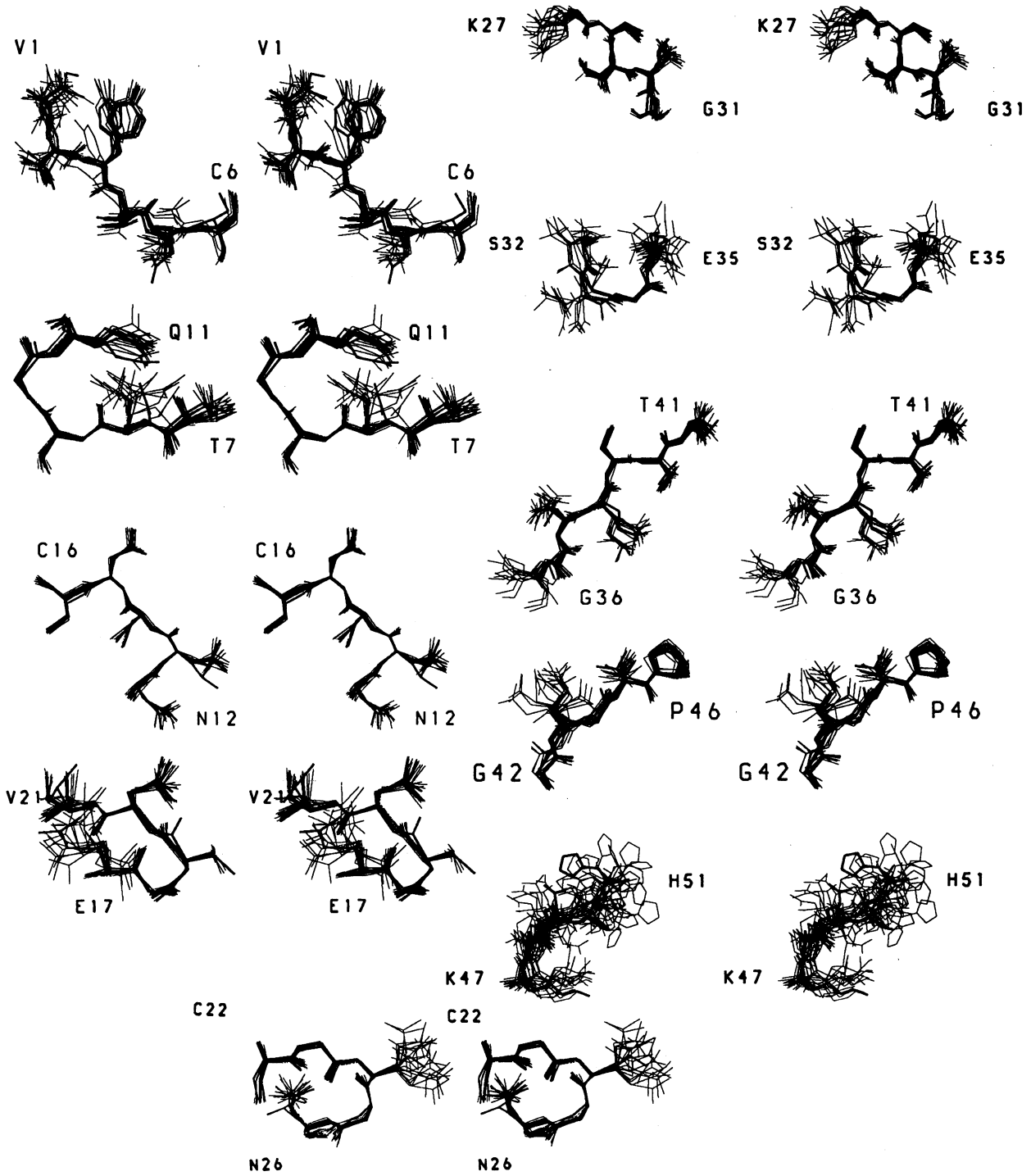

Figure 4. Stereo pictures of the all heavy atom representation of the 20 energy-refined DIANA conformers of hirudin(1-51) (thin lines) superimposed with the hirudin variant HV2-K47 (Scharf *et al.*, 1989) in the hirudin–thrombin complex (bold line) for minimal r.m.s.d. of the backbone atoms N, C^{α} and C′ of the individual segments shown. The following segments are shown: $V(I)_1V(T)VTDC_6$, T_7ESGQ_{11}, $N_{12}LCLC_{16}$, $E_{17}GSNV_{21}$, $C_{22}GQ(K)GN_{26}$, $K_{27}CILG_{31}$, $S_{32}D(N)GE(K)_{35}$, $K(G)_{36}NQCVT_{41}$, $G_{42}EGTP_{46}$, $K_{47}PQ(E)SH_{51}$, where the letters in parentheses indicate the amino acid substitutions in the hirudin variant HV2-K47. Since the co-ordinates of residues 32 to 35 of hirudin are not reported in the X-ray crystal structure (Rydel *et al.*, 1990, 1991), only the 20 energy-refined DIANA conformers are shown for this segment.

segment (Fig. 2) show that they are highly disordered, similar to previous observations for the intact hirudin polypeptide chain (Clore *et al.*, 1987; Folkers *et al.*, 1989; Haruyama & Wüthrich, 1989). Table 4 shows that a total of 15 backbone–backbone hydrogen bonds were identified in hirudin(1-51), of which five are located in β-sheets and one is present in a type II′ turn. The other hydrogen bonds are formed between residues that are located in different secondary structure elements.

For the amino acid side-chains, the all heavy atom superpositions of the 20 energy-minimized DIANA conformers in Figure 4 and the local side-chain displacements, D_{loc}, in Figure 2C show that there are wide variations in the precision of the structure determination for different residues. We somewhat arbitrarily identified 20 "best-defined" residues, i.e. 2, 4, 5, 6, 7, 9, 12, 14, 15, 16, 19, 20, 22, 26, 28, 29, 39, 40, 46 and 48, for which the local side-chain displacement values are below 0·75 Å. Individual stereospecific assignments were obtained for all β-methylene protons and isopropyl methyl groups in these side-chains (Table 1). With the exception of Val2, all best-defined residues exhibit also small backbone displacements. The global r.m.s.d. value calculated for the backbone atoms of residues 3 to 30 and 37 to 48 plus the side-chain heavy atoms of the best-defined among these residues is only slightly larger than the value obtained when only backbone atoms are considered. In contrast, the r.m.s.d. value increases significantly when all heavy atoms of residues 3 to 30 and 37 to 48 are taken into account (Table 3). No significant correlation between the precision of the structure determination and the hydrophobicity or surface accessibility of the individual residues, which was calculated with a modified version of the program ANAREA (Billeter *et al.*, 1990; Richmond, 1984), could be detected. Three hydrogen bonds involving side-chains could be identified (Table 4). The side-chain amide protons of Asn20 interact with the backbone oxygen atom of Glu17, the backbone amide proton of Leu30 is hydrogen-bonded to the oxygen atom of the hydroxyl group of Ser9, and there is a hydrogen bond between the backbone amide proton of Cys39 and the side-chain carboxyl group of Glu17. A high population of this last hydrogen bond has independently been implicated by studies of the pH-dependence of the chemical shift of the Cys39 amide proton (Haruyama *et al.*, 1989; Szyperski, 1992).

Table 4

Hydrogen bonds identified in the 20 energy-minimized DIANA conformers of hirudin(1-51) used to describe the solution structure and in the corresponding polypeptide segment in the X-ray crystal structure of a hirudin–thrombin complex

Donor†	Acceptor†	NMR solution structure‡	X-ray crystal structure§
Cys6 NH	Leu15 O′	5	1
Thr7 NH	Gln11 εO	5	1
Glu8 NH	Gln11 εO	3	1
Gly10 NH	Cys28 O′	20	1
Asn12 NH	Thr45 O′	20	1
Leu13 NH	Cys22 O′	20	1
Leu15 NH	Thr4 O′	20	1
Cys16 NH	Asn20 O′	15	1
Asn20 NH	Glu17 O′	19	0
Asn20 δNH_2	Glu17 O′	11	1
Cys22 NH	Cys14 O′	20	1
Lys27 NH	Val40 O′	20	1
Cys28 NH	Gln11 O′	20	0‖
Ile29 NH	Gln38 O′	20	1
Leu30 NH	Ser9 γO	20	1
Gln38 NH	Ile29 O′	20	1
Cys39 NH	Glu17 εO	12	1
Val40 NH	Lys27 O′	20	1
Gly42 NH	Gly25 O′	20	1
Thr45 NH	Gly10 O′	12	1
Lys47 NH	Asn12 O′	11	1
Lys47 ζNH_3^+	Thr4 γO	7	1
Lys47 ζNH_3^+	Asp5 O′	4	1

† Hydrogen bonds are listed if the donor proton involved forms a hydrogen bond in at least 10 of the 20 energy-minimized DIANA conformers, or if a hydrogen bond was identified in the crystal structure of the hirudin–thrombin complex (Rydel *et al.*, 1990). NH and O′ identify backbone atoms. Side-chain atoms are indicated by Greek letters.

‡ The number of energy-refined DIANA conformers is listed in which the hydrogen bond was identified. The criteria used for the identification of hydrogen bonds are that the proton-acceptor distance must be less than 2·4 Å and the angle between the donor-proton bond and the line connecting the acceptor and donor atoms less than 35°. This criterion is sufficiently loose to detect bifurcated hydrogen bonds.

§ The number 1 indicates the presence of a hydrogen bond in the X-ray crystal structure of the hirudin–thrombin complex reported by Rydel *et al.* (1991) identified with the same geometric criteria as those described above for the energy-refined DIANA conformers. The number 0 indicates that a hydrogen bond implicated by the NMR solution data is not present in the crystal structure.

‖ A hydrogen bond of this type has been reported by Rydel *et al.* (1991) for the X-ray crystal structure of their hirudin–thrombin complex, but these authors used a slightly different search criterion for hydrogen bonds.

4. Discussion

(a) *Comparison of the NMR solution structures of hirudin(1-51), natural hirudin and recombinant desulfatohirudin*

The NMR structures of natural hirudin (Clore *et al.*, 1987), recombinant hirudin (Folkers *et al.*, 1989; Haruyama & Wüthrich, 1989) and recombinant hirudin (Lys47 → Glu) (Folkers *et al.*, 1989) have in common that the N-terminal 48 residues form a compact globular core, while the C-terminal polypeptide 49–65 is flexibly disordered. These earlier structure determinations of intact hirudins do not have the high quality of the structure determination of hirudin(1-51), both because the NMR signals from the flexible C-terminal tail interfere with the analysis of those of the protein core, and because the methodology of NMR structure determination was less advanced several years ago. The improved quality of the present structure determination may be documented with the following data. (1) The number of meaningful NOE upper distance limits for residues 1 to 51 was increased by more than 40% when compared with the data set reported by Haruyama & Wüthrich (1989) for recombinant desulfatohirudin. (2) The number of stereospecific assignments is twice as high as in the data set obtained by Folkers *et al.* (1989) for wild-type recombinant desulfatohirudin. (3) The solution structure of hirudin(1-51) exhibits improved consistency with the experimental constraints when compared with the previous structure determinations of hirudin so that, for example, the average

number of upper distance limit violations per conformer exceeding 0·1 Å decreased from 34 in the structure determination reported by Haruyama & Wüthrich (1989) to 0·3 for hirudin(1-51), or the r.m.s. of the violations of all upper distance bounds decreased from 0·09 Å in the structure of wild-type recombinant desulfatohirudin reported by Folkers *et al.* (1989) to 0·02 Å in hirudin(1-51). It is also worth mentioning that the presently determined solution structure of hirudin(1-51) shows smaller deviations from the corresponding polypeptide segment in the crystal structure of a hirudin–thrombin complex (Table 3) than the NMR structures determined with intact hirudins. The r.m.s.d. values calculated for residues 3 to 30 and 37 to 48 between this crystal structure and the NMR structure reported by Folkers *et al.* (1989) are 0·82 Å for the backbone atoms and 1·44 Å for all heavy atoms, and the corresponding r.m.s.d. values for the structure reported by Haruyama & Wüthrich (1989) are 1·13 Å and 1·48 Å, respectively. Overall, however, the quality of all these structure determinations is sufficiently high to establish unambiguously that the globular core formed by residues 3 to 48 has the same architecture in the intact hirudins and in hirudin(1-51). This is independently supported by the near-identity of corresponding chemical shifts in desulfatohirudin (Folkers *et al.*, 1989; Haruyama & Wüthrich, 1989) and hirudin(1-51) (Table 1), and by the close agreement between the exchange rates of corresponding amide protons in the two proteins (Fig. 5). These observations indicate that the removal of the flexible C-terminal polypeptide segment 52–65, which contains a total of seven carboxyl groups and no basic side-chain, hardly affects the static or dynamic properties of the core structure. This point has been followed up elsewhere (Szyperski, 1992). Here, we make use of these data with the assumption that hirudin(1-51) is a valid representation of the corresponding polypeptide segment of intact hirudin.

(b) *Comparison of the NMR solution structure of hirudin(1-51) with the corresponding polypeptide segment in the crystal structure of a hirudin complex with thrombin*

Although the hirudin(1-51) used in the present study is derived from the hirudin variant HV1 (Scharf *et al.*, 1989) and differs from hirudin HV2-K47 (Harvey *et al.*, 1986), which was used in determining the X-ray crystal structure of the desulfatohirudin–thrombin complex by Rydel *et al.* (1990, 1991), by the seven amino acid substitutions Val1 → Ile, Val2 → Thr, Glu24 → Lys, Asp33 → Asn, Glu35 → Lys, Lys36 → Gly and Gln49 → Glu, it is readily apparent from the available data that the two structures are closely similar. Thus, the r.m.s.d. value between the backbone atoms of residues 3 to 30 and 37 to 48 in hirudin(1-51) in solution and the corresponding atoms in the crystal structure of the desulfatohirudin–thrombin complex is only 0·61 Å (Table 3). Further coincidence is found for residues

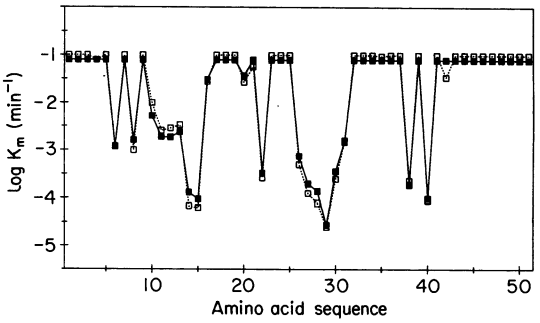

Figure 5. Plot *versus* the amino acid sequence of the rates of backbone amide proton exchange with the solvent at p^{2}H 4·5 and 22°C. Open squares: data for intact recombinant desulfatohirudin (from Haruyama *et al.*, 1989); filled squares: hirudin(1-51).

32 to 35 in the loop formed by residues 31 to 36, which is on the one hand not well determined by the NMR data and on the other hand not visible in the electron density map of the complex (Rydel *et al.*, 1990). The global backbone displacements (Fig. 2A) show that the backbone conformation of the two structures is almost identical for residues 4 to 9, 12 to 17, 22 to 28 and 38 to 48, whereas larger differences are observed for residues 1 to 3, 10 to 11, 17 to 21, 29 to 31 and 36 to 37, where the latter two segments flank the aforementioned region 32–35. The comparison of the backbone dihedral angles ϕ and ψ (Fig. 3) reveals that the minimal deviation between an energy-minimized DIANA conformer and the crystal structure exceeds 20° only for ϕ of Asn20 and Lys36, and for ψ of Tyr3 and Ser19. Moreover, all backbone–backbone hydrogen bonds (Table 4) identified in the N-terminal domain (1-51) of hirudin in the crystal structure of the thrombin complex are present in at least ten of the 20 energy-refined DIANA conformers of Table 2, the sole exception being the hydrogen bond between Cys6 and Leu15, which is found in only five of these solution conformers.

Numerous side-chain conformations are also very similar in the solution and the crystal structure, as can be seen from the superpositions in Figure 4 and the low r.m.s.d. value of 0·91 Å for all heavy atoms of residues 3 to 30 and 37 to 48 (Table 3). The local side-chain displacements (Fig. 2C) between the two structures are within 0·5 Å of the corresponding average local side-chain displacements between the 20 energy-minimized DIANA conformers and the mean solution conformation for all residues except Thr7, Leu15, Ser19, Val21 and Asn26. For these five residues, which all are well defined in both structures, the χ^1 angle in the crystal structure is clearly outside of the χ_1 angle range covered by the 20 energy-minimized DIANA conformers (Fig. 3). Seven intramolecular hydrogen bonds with side-chains are observed in hirudin bound to thrombin (Table 4), three of which are present in solution. The hydrogen bonds of the ζ amino group of Lys47 with the γ hydroxyl group of Thr4 and the backbone

carbonyl oxygen atom of Asp5, which constitute a contact between the N terminus and the C terminus (Rydel *et al.*, 1991), are present in only seven and four DIANA conformers, respectively. Nevertheless, although it does not conform to the hydrogen bond criteria very well, at least the hydrogen bond involving Thr4 seems to be a feature also of the solution structure. This is implicated by the facts that the side-chain orientations of Thr4 in solution and in the complex coincide almost perfectly (Fig. 4), with a small local side-chain displacement (Fig. 2C) and virtually identical χ^1 angles (Fig. 3). Moreover, the side-chain of Lys47 in the complex is located close to the bundle of side-chain orientations in the 20 energy-refined DIANA conformers (Fig. 4). With few exceptions, the well-defined side-chains in the NMR structure, which mostly also agree well with the crystal structure, are located in the core of the molecule. Figures 3 and 4 further show that hirudin(1-51) contains numerous disordered surface side-chains, for which the conformational state cannot be readily compared with the crystal structure.

Overall, using the high-quality NMR solution structure of hirudin(1-51) presented in this paper as a reference, an amazingly close coincidence with the three-dimensional structure of the hirudin polypeptide segment 1-51 in the X-ray crystal structure of the thrombin complex with recombinant HV2-K47 (Rydel *et al.*, 1991) was observed. The near-identity of the global features of the two structures further enabled the identification of subtle local structural differences between free and complexed hirudin. In the accompanying paper (Szyperski *et al.*, 1992*b*) these structural differences are further analyzed with respect to correlations with protein–protein contacts within the thrombin complex as well as additional contacts in the crystal lattice, and implications for the mechanism of hirudin action are discussed.

We thank Dr M. Billeter for helpful discussions and the Schweizerischer Nationalfonds for financial support (project 31.25174.88). The use of the Cray Y-MP of the ETH Zürich is gratefully acknowledged. T.S. is indebted to the Stipendien-Fonds im Verband der Chemischen Industrie for a scholarship. We thank Mr R. Marani for the careful processing of the manuscript.

References

Anil-Kumar, Ernst, R. R. & Wüthrich, K. (1980). A two-dimensional nuclear Overhauser enhancement (2D NOE) experiment for the elucidation of complete proton-proton cross-relaxation networks in biological macromolecules. *Biochem. Biophys. Res. Commun.* **95**, 1–6.

Anil-Kumar, Wagner, G., Ernst, R. R. & Wüthrich, K. (1981). Buildup rates of the nuclear Overhauser effect measured by two-dimensional proton magnetic resonance spectroscopy: implications for studies of protein conformation. *J. Amer. Chem. Soc.* **103**, 3654–3658.

Billeter, M., Braun, W. & Wüthrich, K. (1982). Sequential resonance assignments in protein ^{1}H nuclear magnetic resonance spectra. Computation of sterically allowed proton-proton distances and statistical analysis of proton-proton distances in single crystal protein conformations. *J. Mol. Biol.* **155**, 321–346.

Billeter, M., Kline, A. D., Braun, W., Huber, R. & Wüthrich, K. (1989). Comparison of the high-resolution structures of the α-amylase inhibitor tendamistat determined by nuclear magnetic resonance in solution and by X-ray diffraction in single crystals. *J. Mol. Biol.* **206**, 677–687.

Billeter, M., Schaumann, T., Braun, W. & Wüthrich, K. (1990). Restrained energy refinement with two different algorithms and force fields of the structure of the α-amylase inhibitor tendamistat determined by NMR in solution. *Biopolymers*, **29**, 695–706.

Bode, W., Mayr, I., Baumann, U., Huber, R., Stone, S. R. & Hofsteenge, J. (1989). The refined 1·9 Å crystal structure of human α-thrombin: interaction with D-Phe-Pro-Arg chloromethylketone and significance of the Tyr-Pro-Pro-Trp insertion segment. *EMBO J.* **8**, 3467–3475.

Braunschweiler, L., Bodenhausen, G. & Ernst, R. R. (1983). Analysis of networks of coupled spins by multiple quantum NMR. *Mol. Phys.* **48**, 535–560.

Chou, P. Y. & Fasman, G. D. (1977). β-Turns in proteins. *J. Mol. Biol.* **115**, 135–175.

Clore, G. M., Sukumaran, D. K., Nilges, M., Zarbock, J. & Gronenborn, A. M. (1987). The conformation of hirudin in solution: a study using nuclear magnetic resonance, distance geometry and restrained molecular dynamics. *EMBO J.* **6**, 529–539.

Crawford, J. L., Lipscomb, W. N. & Schellman, C. G. (1973). The reverse turn as a polypeptide conformation in globular proteins. *Proc. Nat. Acad. Sci., U.S.A.* **70**, 538–542.

De Marco, A. & Wüthrich, K. (1976). Digital filtering with a sinusoidal window function: an alternative technique for resolution enhancement in FT NMR. *J. Magn. Reson.* **24**, 201–204.

Dennis, S., Wallace, A., Hofsteenge, J. & Stone, S. R. (1990). Use of fragments of hirudin to investigate thrombin-hirudin interaction. *Eur. J. Biochem.* **188**, 61–66.

Dodt, J., Seemüller, V., Maschler, R. & Fritz, H. (1985). The complete covalent structure of hirudin. Localization of the disulfide bonds. *Biol. Chem. Hoppe-Seyler*, **366**, 379–385.

Eccles, C., Güntert, P., Billeter, M. & Wüthrich, K. (1991). Efficient analysis of protein 2D NMR spectra using the software package EASY. *J. Biomol. NMR.* **1**, 111–130.

Folkers, P. J. M., Clore, G. M., Driscoll, P. C., Dodt, J., Köhler, S. & Gronenborn, A. M. (1989). Solution structure of recombinant hirudin and the Lys47-Glu mutant: a nuclear magnetic resonance and hybrid geometry-dynamical simulated annealing study. *Biochemistry*, **28**, 2601–2617.

Gordon, S. L. & Wüthrich, K. (1978). Transient proton-proton Overhauser effects in horse ferrocytochrome *c*. *J. Amer. Chem. Soc.* **100**, 7094–7096.

Griesinger, C., Sørensen, O. W. & Ernst, R. R. (1985). Two-dimensional correlation of connected NMR transitions. *J. Amer. Chem. Soc.* **107**, 6394–6396.

Griesinger, C., Otting, G., Wüthrich, K. & Ernst, R. R. (1988). Clean TOCSY for ^{1}H spin system identification in macromolecules. *J. Amer. Chem. Soc.* **110**, 7870–7872.

Grütter, M. G., Priestle, J. P., Rahuel, J., Grossenbacher, H., Bode, W., Hofsteenge, J. & Stone, S. R. (1990). Crystal structure of the thrombin-hirudin complex: a

novel mode of serine protease inhibition. *EMBO J.* **9**, 2361–2365.

Güntert, P. & Wüthrich, K. (1991). Improved efficiency of protein structure calculations from NMR data using the program DIANA with redundant dihedral angle constraints. *J. Biomol. NMR.* **1**, 447–456.

Güntert, P. & Wüthrich, K. (1992). A new procedure for high-quality baseline correction of two- and higher-dimensional NMR spectra. *J. Magn. Reson.* **96**, 403–407.

Güntert, P., Billeter, M., Braun, W. & Wüthrich, K. (1989). Automated stereospecific ^{1}H NMR assignments and their impact on the precision of protein structure determinations in solution. *J. Amer. Chem. Soc.* **111**, 3997–4004.

Güntert, P., Braun, W. & Wüthrich, K. (1991*a*). Efficient computation of three-dimensional protein structures in solution from nuclear magnetic resonance data using the program DIANA and the supporting programs CALIBA, HABAS and GLOMSA. *J. Mol. Biol.* **217**, 517–530.

Güntert, P., Qian, Y. Q., Otting, G., Müller, M., Gehring, W. & Wüthrich, K. (1991*b*). Structure determination of the *Antp*(C39 → S) homeodomain from nuclear magnetic resonance data in solution using a novel strategy for the structure calculation with the programs DIANA, CALIBA, HABAS and GLOMSA. *J. Mol. Biol.* **217**, 531–540.

Haruyama, H. & Wüthrich, K. (1989). Conformation of recombinant desulfatohirudin in aequeous solution determined by nuclear magnetic resonance. *Biochemistry,* **28**, 4301–4312.

Haruyama, H., Qian, Y. Q. & Wüthrich, K. (1989). Static and transient hydrogen-bonding interactions in recombinant desulfatohirudin studied by ^{1}H nuclear magnetic resonance measurements of amide proton exchange rates and pH-dependent chemical shifts. *Biochemistry,* **28**, 4312–4317.

Harvey, R. P., Degryse, E., Stefani, L., Schamber, F., Cazeneve, J.-P. (1986). Cloning and expression of a cDNA coding for the anticoagulant hirudin from the bloodsucking leech, *Hirudo medicinalis. Proc. Nat. Acad. Sci., U.S.A.* **83**, 1084–1088.

Johnson, P. H., Sze, P., Winant, R., Payne, P. W. & Lazar, J. B. (1989). Biochemistry and genetic engineering of hirudin. *Sem. Thromb. Hemost.* **15**, 302–315.

Kraulis, P. J. (1991). MOLSCRIPT: a program to produce both detailed and schematic plots of protein structures. *J. Appl. Crystallogr.* **24**, 946–950.

Lent, C. (1986). New medical & scientific uses of the leech. *Nature (London),* **323**, 494–494.

Marion, D. & Wüthrich, K. (1983). Application of phase sensitive two-dimensional correlated spectroscopy (COSY) for measurements of ^{1}H-^{1}H spin-spin coupling constants in proteins. *Biochem. Biophys. Res. Commun.* **113**, 967–974.

Marion, D., Ikura, K. & Bax, A. (1989*a*). Improved solvent suppression in one- and two-dimensional NMR spectra by convolution of time-domain data. *J. Magn. Reson.* **84**, 425–430.

Marion, D., Ikura, K., Tschudin, R. & Bax, A. (1989*b*). Rapid recording of 2D NMR spectra without phase cycling: application to the study of hydrogen exchange in proteins. *J. Magn. Reson.* **85**, 393–399.

Märki, W. E. & Wallis, R. B. (1990). The anticoagulant and antithrombotic properties of hirudins. *Thromb. Haemost.* **64**, 344–348.

Markwardt, F. (1970). Hirudin as an inhibitor of thrombin. *Methods Enzymol.* **19**, 924–932.

Müller, N., Ernst, R. R. & Wüthrich, K. (1986). Multiple-quantum-filtered two-dimensional correlated NMR spectroscopy of proteins. *J. Amer. Chem. Soc.* **108**, 6482–6492.

Nagayama, K. & Wüthrich, K. (1981). Structural interpretation of vincinal proton-proton coupling constants $^3J_{\alpha\beta}$ in the basic pancreatic trypsin inhibitor measured by two-dimensional J-resolved NMR spectroscopy. *Eur. J. Biochem.* **115**, 653–657.

Otting, G. (1990). Zero-quantum suppression in NOESY and experiments with a z filter. *J. Magn. Reson.* **86**, 496–508.

Otting, G., Orbons, L. P. M. & Wüthrich, K. (1990). Suppression of zero-quantum coherence in NOESY and soft-NOESY. *J. Magn. Reson.* **89**, 423–430.

Rance, M., Sørensen, O. W., Bodenhausen, G., Wagner, G., Ernst, R. R. & Wüthrich, K. (1983). Improved spectral resolution in COSY ^{1}H NMR spectra of proteins via double quantum filtering. *Biochem. Biophys. Res. Commun.* **117**, 479–485.

Richmond, T. J. (1984). Solvent accessible surface area and excluded volume in proteins. Analytical equations for overlapping spheres and implications for the hydrophobic effect. *J. Mol. Biol.* **178**, 63–89.

Rydel, T. J., Ravichandran, K. G., Tulinsky, A., Bode, W., Huber, R., Roitsch, C. & Fenton, J. W., II (1990). The structure of a complex of recombinant hirudin and human α-thrombin. *Science,* **249**, 277–280.

Rydel, T. J., Tulinsky, A., Bode, W. & Huber, R. (1991). Refined structure of the hirudin–thrombin complex. *J. Mol. Biol.* **221**, 583–601.

Sasisekharan, V. (1959). Structure of poly-L-proline II. *Acta Crystallogr.* **12**, 897–903.

Scharf, M., Engels, M. & Tripier, D. (1989). Primary structures of new 'Iso-hirudins'. *FEBS Letters,* **255**, 105–110.

Singh, U. C., Weiner, P. K., Caldwell, J. W. & Kollman, P. A. (1986). Amber 3.0, University of California, San Francisco.

Stone, S. R. & Hofsteenge, J. (1986). Kinetics of the inhibition of thrombin by hirudin. *Biochemistry,* **25**, 4622–4624.

Szyperski, T. (1992). Charakterisierung der strukturellen Eigenschaften von Hirudin in Lösung sowie Entwicklung und Anwendung neuer NMR–Methoden zur Untersuchung von Proteinen in Lösung. Ph.D. thesis, ETH-Zürich, Switzerland.

Szyperski, T., Güntert, P., Otting, G. & Wüthrich, K. (1992*a*). Determination of scalar coupling constants by inverse Fourier transformation of in-phase multiplets. *J. Magn. Reson.* In the press.

Szyperski, T., Güntert, P., Stone, S. R., Tulinsky, A., Bode, W., Huber, R. & Wüthrich, K. (1992*b*). Impact of protein-protein contacts on the conformation of hirudin in the X-ray crystal structure of a complex with thrombin studied by comparison with the NMR solution structure of hirudin(1-51). *J. Mol. Biol.* **228**, 1206–1211.

Wagner, G. & Wüthrich, K. (1979). Truncated driven nuclear overhauser effect (TOE). A new technique for studies of selective ^{1}H-^{1}H Overhauser effects in the presence of spin diffusion. *J. Magn. Reson.* **33**, 675–680.

Wagner, G. & Wüthrich, K. (1982). Sequential resonance assignments in protein ^{1}H nuclear magnetic resonance spectra. Basic pancreatic trypsin inhibitor. *J. Mol. Biol.* **155**, 347–366.

Wider, G., Lee, K. H. & Wüthrich, K. (1982). Sequential resonance assignments in protein ^{1}H nuclear mag-

netic resonance spectra. Glucagon bound to perdeuterated dodecylphosphocholine micelles. *J. Mol. Biol.* **155**, 367–388.

Widmer, H., Billeter, M. & Wüthrich, K. (1989). Three-dimensional structure of the neurotoxin ATX Ia from *Anemonia sulcata* in aequeous solution determined by nuclear magnetic resonance spectroscopy. *Proteins,* **6**, 357–371.

Williamson, M. P., Havel, T. F. & Wüthrich, K. (1985). Solution conformation of proteinase inhibitor IIa from bull seminal plasma by ^{1}H nuclear magnetic resonance and distance geometry. *J. Mol. Biol.* **182**, 295–315.

Wüthrich, K. (1986). *NMR of Proteins and Nucleic Acids,* Wiley, New York.

Wüthrich, K., Wider, G., Wagner, G. & Braun, W. (1982). Sequential resonance assignments as a basis for determination of spatial protein structures by high resolution proton nuclear magnetic resonance. *J. Mol. Biol.* **155**, 311–319.

Wüthrich, K., Billeter, M. & Braun, W. (1983). Pseudo-structures for the 20 common amino acids for use in studies of protein conformations by measurements of intramolecular proton-proton distance constraints with nuclear magnetic resonance. *J. Mol. Biol.* **169**, 949–961.

Yonath, A. & Traub, W. (1969). Polymers of tripeptides as collagen models. IV. Structure of poly(L-prolyl-glycyl-L-proline). *J. Mol. Biol.* **43**, 461–477.

Edited by P. E. Wright